A&A 399, 1101–1107 (2003)
DOI: 10.1051/0004-6361:20021831

Astronomy & Astrophysics

Compositional dependence of infrared absorption spectra of crystalline silicate

II. Natural and synthetic olivines

C. Koike[1], H. Chihara[1,2], A. Tsuchiyama[2], H. Suto[3], H. Sogawa[1], and H. Okuda[4]

[1] Kyoto Pharmaceutical University, Yamashina, Kyoto 607-8412, Japan
[2] Department of Earth and Space Science, Osaka University, Toyonaka, Osaka 560-0043, Japan
[3] Subaru Telescope, National Astronomical Observatory of Japan, Hilo, Hawaii, USA
[4] Gunma Astronomical Observatory, Agatsuma, Gunma 377-0702, Japan

Received 30 July 2002 / Accepted 10 December 2002

Abstract. The mass absorption spectra of crystalline olivine particles with different Mg/(Mg + Fe) ratios, between forsterite (Mg_2SiO_4, Fo) and fayalite (Fe_2SiO_4, Fa), were measured for synthetic and natural samples in the mid- and far-infrared regions. The main strong peaks show a systematic shift to longer wavelengths as the Mg/(Mg + Fe) ratio decreases. In the 10–17 μm region, these trends are very clear, and the peak positions are a good indicator of the composition of dust grains. In the 20–100 μm region, the trends are also rather clear, though they are slightly complicated; the intensity and width of the various bands become weak and broad, respectively, or the bands disappear as the concentration of Fo decreases. However, the trends are clear only in a limited composition range near Fo and Fa; the peak positions of 30, 50, and 69 μm bands of forsterite shift linearly as the Fo concentration decreases to about Fo_{70}. Those of the double band in the 50 μm region for Fe-rich olivine shift linearly as the Fa concentration increases from Fo_{20} to Fa. When the spectral signature of Mg-rich or Fe-rich olivine can be observed, the peak positions in the 20–100 μm region are a good indicator of the composition of dust grains.

Key words. methods: laboratory – interplanetary medium – star: circumstellar matter – ISM: dust, extinction – ISM: lines and bands – infrared: ISM

1. Introduction

In addition to the characteristic 11.2–11.3 μm band of olivine in many comets such as Halley, Bradfield, Levy, and Muller (Hanner et al. 1994), many characteristic features in the far infrared region were observed around the circumstellar environment of both evolved and young stars and the Hale-Bopp comet. The majority of these features were identified with Mg-rich crystalline olivine and pyroxene (Waters et al. 1998; Molster et al. 1999; Crovisier et al. 1997; Malfait et al. 1998; Wooden et al. 1999; Molster et al. 2002a,b). Further, the detected 69 μm feature in the ISO spectra led to the conclusion that the crystalline olivine is also very Mg-rich comparing with laboratory data dependent on the composition and temperature (Molster et al. 2002c). However, no evidence of the presence of iron-rich silicates has been obtained to date. The absence of Fe-rich silicates is very curious as the most abundant elements forming refractory compounds are Mg, Si, and Fe with oxygen. A model of the evolution of mineral dust grains in the circumstellar environment has been discussed; at low temperature after condensation of forsterite and enstatite, gaseous Fe reacts with Mg-rich silicates and amorphous Fe-rich olivines may condensate (Tielens et al. 1998), or the olivine grains develop a core mantle structure with an Mg-rich olivine in the core and Fe-rich olivine in the mantle, and the remaining fraction of the iron forms metallic iron grains (Gail & Sedlemeyer 1999). The spectra of crystalline silicates dependent on the Mg/(Mg + Fe) ratio is a key to understanding the structure, origin, and evolution of circumstellar and interstellar dust, and possibly to identifying the chemical condensation path of circumstellar minerals. Once the carrier of the observed bands has been identified, laboratory spectra should be carefully compared. Generally speaking, the laboratory spectra vary depending on the chemical composition, temperature, and grain shapes of samples. With regard to laboratory data dependence on composition, we already measured the spectra of olivine with different Mg/(Mg + Fe) ratios, including Fo_{100}, Fo_{90}, Fo_{80}, Fo_{60}, and Fo_{40} (Koike et al. 1993). We have clarified that the peak position of the main bands shifts to a longer wavelength as this ratio decreases. This trend was confirmed for olivine and pyroxene by Jäger et al. (1998), using olivine compositions of Fo_{100}, Fo_{94}, Fo_{55}, and fayalite. Chihara et al. (2002) (Paper I)

Send offprint requests to: C. Koike,
e-mail: koike@mb.kyoto-phu.ac.jp

investigated and confirmed this trend in more detail for Mg-Fe pyroxenes with different Mg/(Mg + Fe) ratios. In previous investigations of the spectra of olivine (Koike et al. 1993; Jäger et al. 1998), the spectra in the far infrared region were found to change drastically between forsterite and fayalite; a single peak of forsterite at 50 μm was changed to double bands of fayalite, and a strong peak of forsterite at 69 μm faded away for fayalite. The significance of these detailed trends, especially near Mg-rich and Fe-rich olivine, is not yet clear. For Fe-rich olivine, only two spectra, that of fayalite and that of Fo_6, by Jäger et al. (1998) and Mennela et al. (1998), respectively, have been measured. Further, the samples synthesized by Jäger et al. (1998) are phase-separated (inhomogeneous) materials. It is advantageous to measure the spectra of homogeneous samples so that they can be used as reference materials for spectroscopy. In order to examine in more detail how these peak positions shift with the Mg/(Mg + Fe) ratios near forsterite and fayalite, we obtained especially Mg-rich olivine and Fe-rich olivine samples. Following our Paper I, we measured the absorption spectra of the whole range of olivine solid solutions from forsterite to fayalite in the mid-infrared region (5–25 μm) and the far-infrared region (longer than 25 μm). Previous data (Koike et al. 1993) in the mid-infrared region had low resolution, and those in 25–35 μm were not smoothly connected with the data in the mid- and the far-infrared region. All these data were re-measured in the present study. We report the spectra of an olivine series, and clarify the correlation between the peak positions and the Mg/(Mg + Fe) ratio in detail.

2. Experiment

Olivine is a solid solution having as its two end members forsterite Mg_2SiO_4 (Fo) and fayalite Fe_2SiO_4 (Fa), and is expressed as $(Mg_x, Fe_{1-x})_2SiO_4$ ($0 \leq x \leq 1$). The composition of olivine is expressed as Fo_X, where X is the mole percentage of forsterite ($X = 100\ x$). In this study, both the synthetic and natural olivines are prepared as listed in Table 1. Synthetic Fo was made by the Czochralski (CZ) method (Takei et al. 1974), and Fa was made by the floating-zone (FZ) method (Takei 1978). The other synthetic olivine samples – Fo80, Fo60, Fo40, Fo20, Fo15, and Fo10 – were produced at 1200 °C by heating a mixture of MgO, SiO_2, and FeO powder under controlled O_2 fugacity at atmospheric pressure. This method is the same as that mentioned in Paper I for synthesizing pyroxenes. None of the samples showed any phase-separated materials or any inhomogeneity under a SEM, based on the finding that the back scattered electron images were uniform.

The composition of olivine samples was determined by an EPMA (electron probe micro analyzer) at Osaka University (JEOL733). For the EPMA investigations, the chemical composition of natural samples are from $Fo_{92.1}$ to Fo_{77} as listed in Table 1. Natural olivines contain minor compounds such as MnO, NiO, and CaO (below 0.2 mol %), and the spectral influence of these minor compounds might be negligible. The samples of AK, Fo80, Fo60, and Fo40 samples, which are the same as those in Koike et al. (1993), were very finely ground. The errors of chemical compositions in these samples are rather large compare to those in other samples, due to the fact that the radius of these particles was rather small relative to the beam radius of the electron. The synthetic Fo, Fa and natural samples are single crystal, whereas other synthetic olivines are polycrystal. The synthesized and natural samples were crushed and ground in an agate mortar. After the large particles had been excluded via sedimentation in alcohol, the fine particles were well mixed with KBr or polyethylene powder in an agate mortar. These fine particles were embedded in KBr or polyethylene. The diameter of the KBr pellets was 13 mm. Polyethylene pellets (sheets) were made after heating the mixture, and the diameters of the pellets were about 20–30 mm according to the total amount of the mixture. The transmittances T of each KBr and polyethylene pellet were measured from 7000 cm^{-1} to 50 cm^{-1}. The spectrometers used were the Jasco FT/IR-350 and the Nicolet FTIR (Nexus 670) at a resolution of 1 cm^{-1}. In the far-infrared region (250–50 cm^{-1}), the spectra were also measured, at the lower resolution of 4 cm^{-1} to avoid interference fringe. The mass absorption coefficient, κ, is derived as

$$\kappa = \frac{S}{M} \ln\left(\frac{1}{T}\right),$$

where S is the surface area of the sample pellet, M is the mass of the sample included in the KBr or polyethylene pellets, and T is the transmittance of the sample pellet. We ascertained the reproduction of the mass absorption coefficients for each sample, changing the ratio of the sample in KBr or polyethylene. The absorption spectra by KBr and polyethylene pellets were smoothly connected, and they overlapped in wide wavelength range from approximately the 17 μm to the 25 μm region. Typically, the present data shorter than 20 μm are from KBr pellets, and those longer than 20 μm are from the polyethylene pellets.

3. Results

The spectra of all samples are shown as mass absorption coefficients κ (cm^2/g) in Fig. 1. The previous data for natural olivine for AK (Ichinomegata Akita, $Fo_{89.3}$) in the far-infrared region (Koike et al. 1993) are also included. The revised peak positions in the mid-infrared region with high resolution (Koike et al. 1993) are blue shifted by about 0.1 $\sim$ 0.2 μm compared with their positions in previous data (Koike et al. 1993).

Peak positions of all samples in μm are listed in Table 2. For all bands, the correlation between the peak positions of each band and the concentration of Fo (mol %), X, is plotted in Fig. 2. Based on Figs. 1 and 2, we examine the peak positions of each band dependent on the chemical composition.

3.1. Peak shifts as Fa content increases

The spectra of the synthetic olivine gradually changed from forsterite to fayalite as the Fe content increased, and this change became distinct in the far-infrared region in particular, as shown in Fig. 1. As for natural olivine, its chemical compositions were limited to a narrow range from $Fo_{92.1}$ to Fo_{77}. The spectra of natural samples were more similar to each other in the mid- and far-infrared regions than to the spectra of synthetic olivine. With regard to the 70 μm band, the peak positions of

Table 1. Natural and synthetic olivine samples.

sample name		chemical composition (mol %) concentration of Fo		minor compounds
natural	location			
KH	Kohistan, Pakistan	92.1 ± 0.3	(30)	MnO≦0.1, NiO≦0.3
SJ	St. Jones Island, Egypt	91.4 ± 0.4	(17)	MnO≦0.1
SC	San Carlos, Arizona, USA	90.7 ± 0.2	(5)	MnO≦0.1, NiO≦0.4
AK *	Ichinomegata, Akita, Japan	89.3	(1)	NiO≦0.3
HW	Black sand beach, Hawaii, USA	86.5 ± 0.3	(14)	MnO≦0.2
MY	Miyake Island, Tokyo, Japan	84.4 ± 0.1	(25)	MnO≦0.2, CaO≦0.2
NS	Nishigatake, Saga, Japan	84.2 ± 0.2	(26)	MnO≦0.2, CaO≦0.2
NV	Nivitigala, Sri Lanka	77	(1)	
synthetic	synthetic method			
Fo	CZ method [1]	———		
Fo80 *	heating at 1200 ℃	75.2 ± 2.4	(3)	
Fo60 *	heating at 1200 ℃	56.8 ± 2.2	(15)	
Fo40 *	heating at 1200 ℃	39.5 ± 2.1	(19)	
Fo20	heating at 1200 ℃	21.8 ± 0.4	(19)	
Fo15	heating at 1200 ℃	15.9 ± 0.2	(31)	
Fo10	heating at 1200 ℃	11.0 ± 0.2	(16)	
Fa	FZ method [2]	———		

*: same sample as in Koike et al. (1993).
[1] : CZ; Czochralski method (Takei et al. 1974).
[2] : FZ; Floating zone method (Takei 1978).
numbers in ( ) of third column are analyzed number.

natural olivine were definitely shifted to a longer wavelength as the Fe content increased.

The trend for each band seemed no different between synthetic and natural olivine; the same symbols are shown in Fig. 2. The sizes of symbols indicate the strength of the peaks. From Fig. 2, the following trends have been found.

(1) All peaks are shifted toward longer wavelengths as the Fo content decreases (i.e., the Fa content increases).

(2) For several strong bands, seen at 11.2, 16.4, and 23.7 μm of Fo, respectively, peak positions are strongly correlated with the Fo content, X. The peak positions in wavenumber (cm^{-1}), ν, are nearly linear with X.

3.2. In the 10–20 μm region

The three peaks of forsterite, at 1000, 893, and 614 cm^{-1} (10, 11.2, and 16.3 μm), are strong, and two peaks, at 962 and 840 cm^{-1} (10.4 and 11.9 μm), are weak. The peak positions of all these bands shift linearly to longer wavelengths as the Fa content increases. Forsterite and all natural olivines have a 500 cm^{-1} (20 μm) band with a shoulder at about 550 cm^{-1} (18 μm). For the Fo80 sample, this 20 μm band is very broad with a single structure. As the Fa content increases below Fo_{60}, this band broadens and splits into a double structure, and Fa sample shows clearly double bands at 508 and 478 cm^{-1} (19.7 and 20.9 μm), respectively.

3.3. In the 20–30 μm region

The strong 422 cm^{-1} (23.7 μm) band (solid square marks in Fig. 2) of forsterite (dotted arrows in Fig. 1) becomes weaker as the Fo content decreases up to the Fo60 sample (including all natural samples). The Fo40 sample shows nearly the same strength as the next band of 345 cm^{-1} (29 μm), whereas below the Fo20 sample this band becomes weaker than the next band of 332 cm^{-1} (30 μm). With regard to the double structure of forsterite at 383 cm^{-1} (26.1 μm) and at 364 cm^{-1} (27.5 μm) (bold arrows in Fig. 1) (full star marks in Fig. 2), natural olivines (KH, SJ, SC, AK, HW) also show a double structure at about 380 and 360 cm^{-1} (26 and 27 μm). This double structure becomes a single band and broadens for the Fo80 sample and natural olivine (MY, NS, NV). This broad band becomes strong and shifts to 313 cm^{-1} (31.9 μm) of fayalite as the Fa content increases. The strong band of 313 cm^{-1} (31.9 μm) of fayalite splits into double bands at 26 and 27 μm for forsterite.

3.4. The 33 μm band

The strong band at 296 cm^{-1} (33.8 μm) with two sharp peaks of forsterite becomes a single band for $Fo_{92.1}$–Fo_{77} composition, and becomes very weak for $Fo_{56.8}$ and $Fo_{39.5}$ composition. The band appears weakly for the Fo10 sample, and for Fa the band appears clearly at 257 cm^{-1} (38.9 μm).

3.5. The 50 μm and 70 μm bands

In the far infrared region, a strong peak appears at 200 cm^{-1} (50 μm) and 144 cm^{-1} (69.6 μm) for forsterite, and these peaks are also sensitive to the chemical composition.

With regard to the 50 μm band, the peak also appears for five natural olivines ($Fo_{92.1}$–$Fo_{86.5}$). In the case of the MY, NS, and NV samples, the 50 μm peak appears, but not clearly.

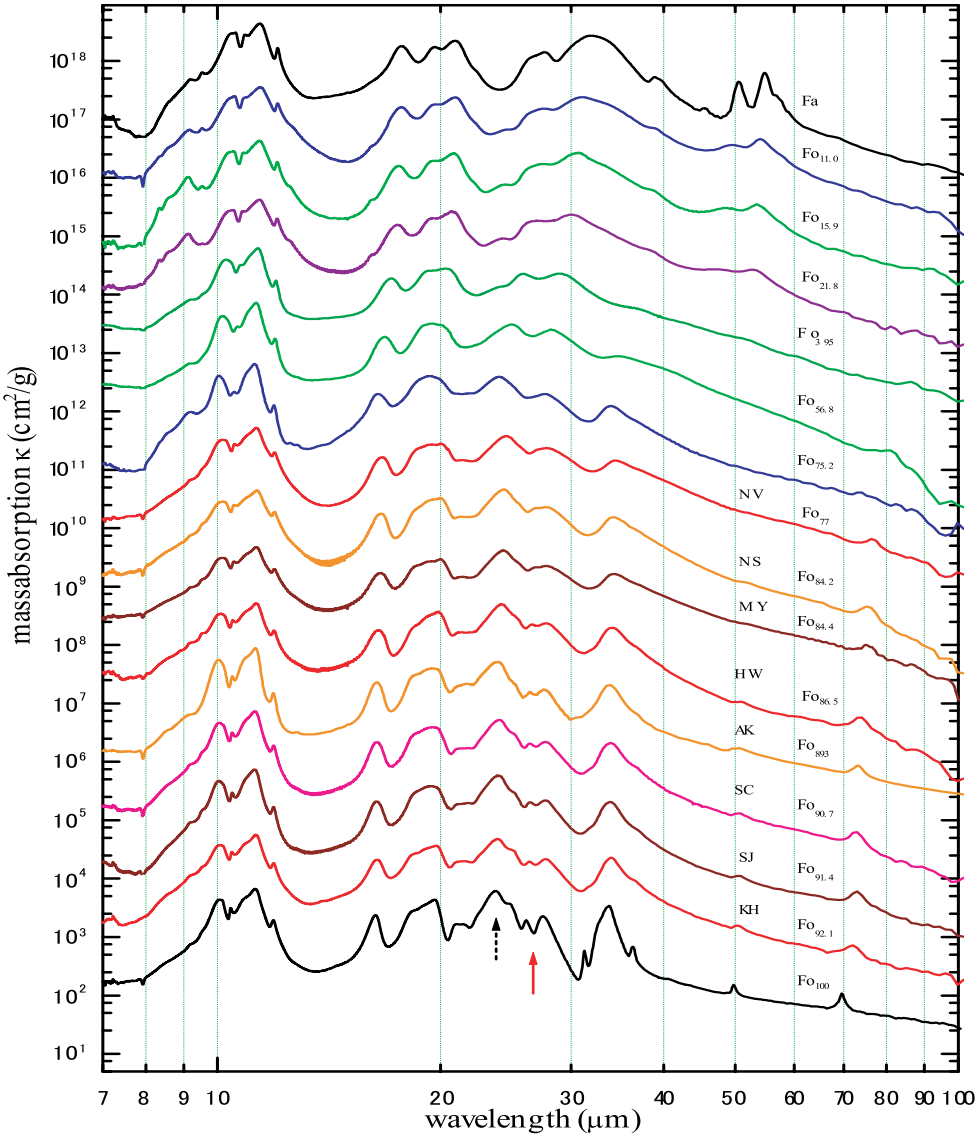

Fig. 1. Spectra of synthetic olivine and natural olivine. Each spectrum, indicating by its composition, is multiplied the under spectrum by 10. The dotted and bold arrows indicate 23.7 μm and the double structure of forsterite, respectively; see Sect. 3.3.

This band does not appear for synthetic olivine (Fo80–Fo40 samples). In the case of the Fo20 sample, very weak double bands appear in the 50 μm region. These double bands become clearer and stronger as the Fa content increases, and for Fa sample two very strong bands appear at 198 and at 183 cm^{-1} (50.6 and 54.7 μm).

With regard to the 70 μm band, forsterite shows a sharp and distinct band at 144 cm^{-1} (69.6 μm). In the case of natural olivine, the 70 μm peak clearly appears, and shifts to 72 μm (KH), 73 μm (SJ and SC), 73.2 μm (AK), 74.1 μm (HW), 74.9 μm (MY), 75.2 μm (NS), and 76.3 μm (NV). Even in the case of NV, which has a Fo_{77} composition, the 70 μm peak clearly appears at 76.3 μm. All natural olivines definitely show this band, and this peak position shifts to the longer wavelength as the Fa content increases. However, all the synthetic olivines except forsterite show this band very weakly beyond 70 μm. The peak position of the fayalite shows much more vaguely at about 103 and 94.3 cm^{-1} (97 and 106 μm), and is not added to the figure due to large errors, whereas the bulk sample of fayalite shows the bands at 94 and 109 μm (Hofmeister et al. 1997). In the far-infrared region, the SiO_4 groups in olivines are distorted, partly due to the influence of Fe incorporation. The small iron content significantly reduces the intensity of some peaks, including those at 33, 50, and 70 μm.

4. Discussions

4.1. Peak shifts depending on bands

The peak positions for forsterite (Fo_{100}), natural olivine (Fo_{94}, Fo_{55}), and fayalite determined by Jäger et al. (1998) are plotted as open circles; those for natural olivine (Fo_{90} and Fo_6) determined by Mennella et al. (1998) as asterisks; and those for forsterite (Fo_{100}) and natural olivine (Fo_{89}) determined by Bowey et al. (2001) as open triangles in Fig. 2. The trends of their data resemble those of ours. Although Jäger et al. (1998) showed forsterite having three bands in the region

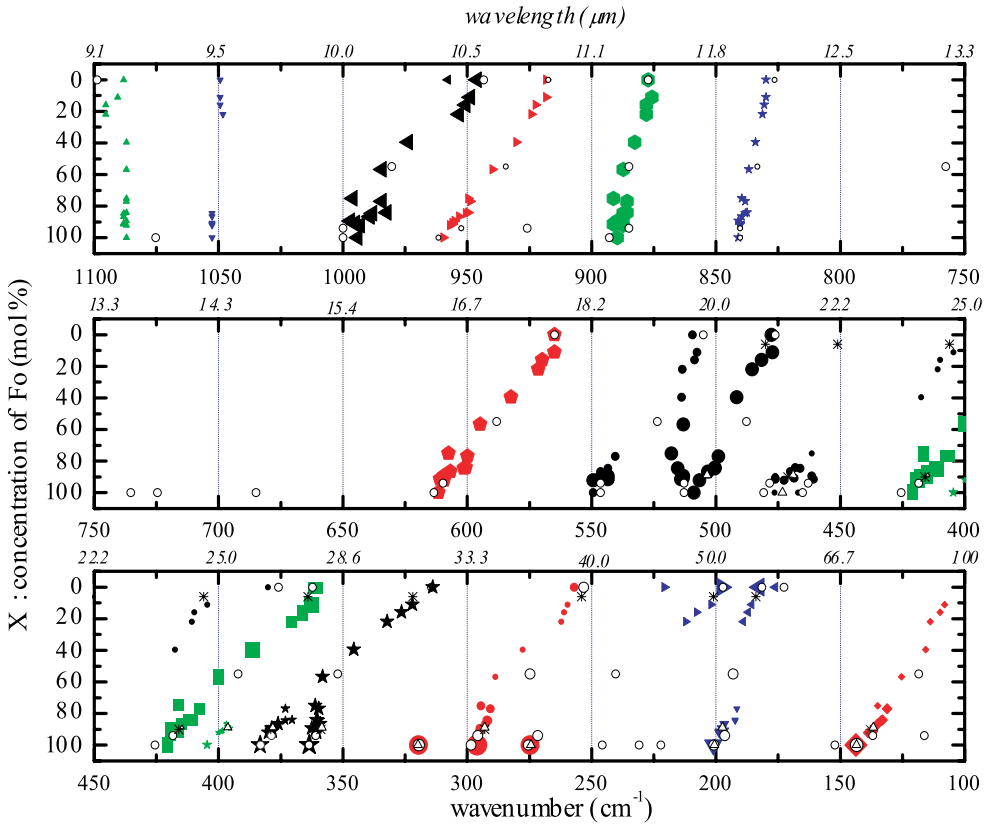

Fig. 2. Peak shifts of absorption bands depending on chemical composition. Solid symbols are synthetic and natural samples. Open circles ○, asterisk ∗, and open triangle △ are from Jäger's (1998), Mennela's (1998), and Bowey's data (2001), respectively. The sizes of the symbols indicate the strength of peaks.

between 40–50 μm, these bands do not appear for our or Bowey's forsterite. Further, Jäger's forsterite has other bands at 13.6, 13.8, 14.6, and 65.7 μm, and these bands do not appear in our or Bowey's forsterite. This difference may be due to the fact that Jäger's forsterite sample was inhomogeneous and some other compounds (or impurity) remain.

From Fig. 2, there seems generally to be no difference between natural and synthetic olivine. The peak positions of each band in wavenumber (cm^{-1}), ν, linearly shift as the Fo content, X, decreases; that is, ν are nearly in proportion to X, although some change appears around chemical composition Fo_{80}–Fo_{70}. The linear fitting equations for the respective bands are listed in Table 3. The proportional coefficients or the slopes between ν and X for each band (ν is proportional to X) that are shown in Fig. 2 and Table 3 evidently differ. For example, the slopes are 0.15 for 11.2 micron band, 0.12 for 12 micron band, 0.51 for 16 micron band, 0.65 for 23.7 micron band, and 0.37 for 70 micron band. These results are different from those determined by Jäger et al. (1998), in which the shifts in wavenumber are constant for the different bands and proportional to the [FeO] content (their slope is 0.56). From Fig. 2 and Table 3, it can be seen that the peak shifts or the slopes are very small for 11.2 and 11.9 micron bands of Fo. For other bands, the peak shifts are very clear, and their slopes are about 0.4–0.7. With regard to the 26.1 and 27.5 micron bands, these double bands become single in the Fo80 sample. Including the medium 26.1 micron band instead of the strong 27.5 micron band for X regions from 100 to 80, the fitting slope becomes 0.68, which is similar to that of the 23.7 micron band.

The positions in the 10–17 μm region are good indicators of the Mg/(Mg + Fe) ratio. However, in the 20–100 μm region, the peak shifts are rather complicated, due to the fact that these bands become weak, broad, or undistinguished as the Fa content increases. Lastly, we discussed the differences in spectra of the 70 μm band between natural and synthetic olivine. All natural olivine samples ($Fo_{92.1}$–Fo_{77}) clearly showed a 70 μm band similar to forsterite. Further, according to Jäger et al. (1998), natural hortonolite (Fo_{55}) shows a weak peak at 84.4 μm. In contrast, synthetic Fo80 and Fo60 samples show a very weak band at 74.1 and 79.8 μm, respectively. These findings might explain differences in crystal state (single crystal or polycrystal), or the preferential concentration of Mg and Fe elements to the M1- or M2-site (Aikawa et al. 1985; Morimoto 1993), but more information is needed and additional measurements of synthetic olivine must be examined.

4.2. The chemical route of silicate formation

Observation by ISO shows that ubiquitous Mg-rich crystalline silicates (forsterite and enstatite) exist in the circumstellar region. Thus far, crystalline fayalite or Fe-rich silicates has not detected by ISO observation. As mentioned in the Introduction, evolution models to explain the absence of Fe-rich silicates in the circumstellar environments have been suggested by

Table 2. Peak positions in μm at room temperature. The first and second lines are the sample name and concentration of Fo (mol %), respectively. $*$: very weak peak.

Fo	KH	SJ	SC	AK	HW	MY	NS	NV	Fo80	Fo60	Fo40	Fo20	Fo15	Fo10	Fa
100	92.1	91.4	90.7	89.3	86.5	84.4	84.2	77	75.2	56.8	39.5	21.8	15.9	11.0	0
9.2*	9.2*	9.2*	9.2*	9.2*	9.2*	9.2*	9.2*	9.2*	9.2	9.2*	9.2*	9.1	9.1	9.2	9.2
9.5*	9.5*	9.5*	9.5*		9.5*	9.5*						9.5*	9.5*	9.5	9.5
															10.4*
10.06	10.16	10.05	10.05	10.03	10.11	10.12	10.18	10.16	10.04	10.16	10.27	10.49	10.52	10.54	10.57
10.42	10.46	10.46	10.46	10.47	10.49	10.52	10.53	10.54	10.53	10.64	10.75	10.82	10.84	10.89	10.89
11.24	11.28	11.22	11.23	11.24	11.27	11.27	11.29	11.29	11.22	11.27	11.33	11.39	11.39	11.42	11.40
11.9	11.9	11.9	11.9	11.9	11.9	11.9	11.9	11.9	11.9	12.0	12.0	12.0	12.0	12.1	12.1
16.4	16.5	16.4	16.4	16.4	16.5	16.6	16.7	16.7	16.5	16.8	17.2	17.5	17.6	17.7	17.7
						18.4*		18.5*							
18.2*	18.3*	18.4*	18.3*	18.4*	18.3*	19.4*					19.5*	19.5	19.7	19.7	19.6
19.7	19.8	19.5	19.5	19.5	19.9	20.0	20.0	20.0	19.3	19.5	20.3	20.6	20.8	21.0	20.9
20.8	21.2*	21*	21*	21*											
21.4*		21.7*	21.3*	21.7*	21.3*	21.5*	21.4*	21.5*	21.7*		24. 0*	24.3*	24.4*	24.7*	26.3*
23.7	24.0	23.9	24.0	23.9	24.1	24.3	24.3	24.6	24.0	25.0	25.9	27.0	27.3	27.6	27.7
24.8		25.1	25.1	25.3	25.2										
26.1	26.3	26.4	26.4	26.4	26.6	26.8*	27.0*	26.8*							
27.5	27.7	27.7	27.7	27.6	27.8	27.8	27.7	27.8	27.7	27.9	28.9	30.1	30.6	31.1	31.9
31.3															
33.8	33.9	33.9	34.0	33.9	34.2	34.3	34.2	34.4	34.0	34.6	36	38.1*	38.3*	38.5*	38.9*
36.4															
															45.3
												47.1*	48.1	49.5	50.6
49.7	50.3	50.3	50.8	50.6	50.8	52*	52*	(52?)							
												52.9*	53.5	53.9	54.7
															56.8*
69.6	72.0	73.0	73.0	73.2	74.1	74.9	75.2	76.3	74.1*	79.8*	86.4*	87.9*	91.0*	92.6*	97*?
															105.8*?

Tielens et al. (1998) and by Gail & Sedlmayr (1999). According to the model by Tielens et al. (1998), if Fe-rich olivine in the circumstellar region crystallizes in response to some annealing mechanism, detection of strong double peaks at 50.6 and 54.8 μm can be expected. According to the model by Gail & Sedlmayr (1999), the average composition x of olivine grains is about 0.7–0.6, and the surface composition of olivine x is about 0.4–0.7 as dependent on the magnitude of the ion exchange coefficient. In the case in which x is 40–70 mole % (i.e., when Fo_{40}–Fo_{70}), there is no feature or there is a very weak peak in the 50 μm and 70 μm regions, respectively, in the present olivine spectra. Determining the spectral signatures of Fe-rich olivine could be resolved this problem. The spectral signatures appear at 50 μm, where there is a strong single peak of forsterite or a double peak of fayalite, and at the 70 μm band, where the peak position shifts to a longer wavelength as the Fo content decreases.

In the case of the 70 μm band, the intensity of natural olivine is weak compared to that of forsterite. Based on the ISO observations of evolved stars, the detected 70 μm band was around 69 μm, and was identified with forsterite, taking into account the temperature dependence (Molster et al. 2002c; Bowey et al. 2001). The peak position of present natural olivine does not shift to below 70 μm, even after cooling to 4 K from the peak shift of natural olivine Fo_{90} at 20 K (Mennela et al. 1998). As mentioned above, the intensity and peak position of this 70 μm band are very sensitive to chemical composition. It is very interesting how the intensity and peak position of the band changed for the limited composition Fo–Fo_{90}. Not only the 70 μm band but also the 33 and 50 μm bands were sensitive to chemical composition and were largely changed near Fo and Fa. The more detailed trends of these bands are interesting, and further investigation of the limited compositions of Fo–Fo_{90} and Fo_{10}–Fa are needed.

4.3. Peak shifts of olivine and pyroxene

For olivine samples, the peak positions in the mid-infrared region shift linearly as Fo concentration decreases, whereas in the far-infrared region this trend appears clearly only near the end members; the peak positions of 33 , 50, and 69 μm bands of Fo clearly shift linearly from Fo to about Fo_{70}, and the peak positions of Fa at 50 μm bands clearly shift linearly as Fa concentartion decreases to about Fo_{20}. In contrast, these trends appear slightly different for pyroxene (Paper I). The compositions of pyroxene are limited to En–En50 and Fs, and the peak shifts

Table 3. The correlation between peak position ν in wavenumber (cm^{-1}) and Fo content, X.

peak band of Fo	linear fitting equation
10 μm	$\nu = 0.53X + 946$
10.4 μm	$\nu = 0.44X + 915$
11.2 μm	$\nu = 0.15X + 876$
11.9 μm	$\nu = 0.12X + 829$
16.3 μm	$\nu = 0.51X + 562$
23.7 μm	$\nu = 0.65X + 359$
27.5 μm	$\nu = 0.48X + 320$
27.5 μm*	$\nu = 0.68X + 316$
33.4 μm	$\nu = 0.43X + 257$
69 μm	$\nu = 0.37X + 104$
50 μm (Fo)	$\nu = 0.48X + 154$
50 μm (Fa)	$\nu = 0.67X + 197$
50 μm (Fa)	$\nu = 0.29X + 183$

Here, as was the case for 27.5 μm*, peaks are fitted including the 26.1 μm band instead of the 27.5 μm band in the range of X from 100 to 80. For 50 μm (Fo) and (Fa), peaks are fitted for the 50 μm bands only for a limited range of X in the case of Fo-rich and Fa-rich olivine, respectively.

in the mid-infrared region do not appear as clearly as those of olivine, whereas the peak shifts in the far-infrared region, especially at around the 40–50 and 70 μm regions, clearly appear. Up to now, crystalline olivine and pyroxene had been detected by ISO observation. This trend in peak shifts of olivine and pyroxene will contribute to identification of the bands and clarify overall chemical composition. In particular, from the peak shifts of olivine in the mid-infrared region and those of pyroxene in the far-infrared region, we can easily determine the chemical composition of crystalline silicates. Spectra with high resolution around the circumstellar environment will provide a clue to clarify the growth of circumstellar dust.

Acknowledgements. We thank Professor H. Takei of Osaka University for preparing Fayalite crystal. This work was supported by a Grant-in-Aid from the Japanese Ministry of Education, Science, and Culture (No. 12440054), and a Research fellowship from the Japan Society for the Promotion of Science for Young Scientists (to Chihara). We thank the referee Dr. J. E. Bowey for constructive comments that have improved this paper. We are grateful to Dr. Catherine Ishida for improving expressions of our manuscript.

References

Aikawa, N., Kumazawa, M., & Tokonami, M. 1985, Phys. Chem. Minerals, 12, 1
Bowey, J. E., Lee, C., Tucker, C., et al. 2001, MNRAS, 325, 886
Chihara, H., Koike, C., Tsuchiyama, A., Tachibana, S., & Sakamoto, D. 2002, A&A, 391, 267 (Paper I)
Crovisier, J., Leech, K., & Bockelee-Morvan, D., et al. 1997, Science 275, 1904
Gail, H.-P., & Sedlmayr, E. 1999, A&A, 347, 594
Hanner, M. S., Lynch, D. K., & Russell, R. W. 1994, ApJ, 425, 274
Hofmeister, A. M. 1997, Phys. Chem. Minerals, 24, 535
Jäger, C., Molster, F. J., Dorschner, J., et al. 1998, A&A, 339, 904
Koike, C., Shibai, H., & Tsuchiyama, A. 1993, MNRAS, 264, 654
Malfait, K., Waelkens, C., Waters, L. B. F. M., et al. 1998, A&A, 332, L25
Mennella, V., Brucato, J. R., Collangeli, L., et al. 1998, ApJ, 496, 1058
Molster, F. J., Waters, L. B. F. M., Trams, N., et al. 1999, A&A, 350, 163
Molster, F. J., Waters, L. B. F. M., Tielens, A. G. G. M., et al. 2002a, A&A, 382, 184
Molster, F. J., Waters, L. B. F. M., & Tielens, A. G. G. M. 2002b, A&A, 382, 222
Molster, F. J., Waters, L. B. F. M., Tielens, A. G. G. M., et al. 2002c, A&A, 382, 241
Morimoto, N. 1993, Rock-forming minerals (Tokyo University press) (in Japanese)
Takei, H. 1978, J. Crystal Growth, 43, 463
Takei, H., Miura, T., & Morioka, M. 1974, J. Cryst. Growth, 23, 121
Tielens, A. G. G. M., Waters, L. B. F. M., Molster, F. J., & Justtanont, K. 1998, Ap&SS, 255, 415
Waters, L. B. F. M., Beintema, D. A., Zijlstra, A. A., et al. 1998, A&A, 331, L61
Wooden, D. H., Harker, D. E., Woodward, C. E., et al. 1999, ApJ, 517, 1034